Volume 7 | Number 2 | 14 January 2015 | Pages 369–844

Nanoscale

www.rsc.org/nanoscale

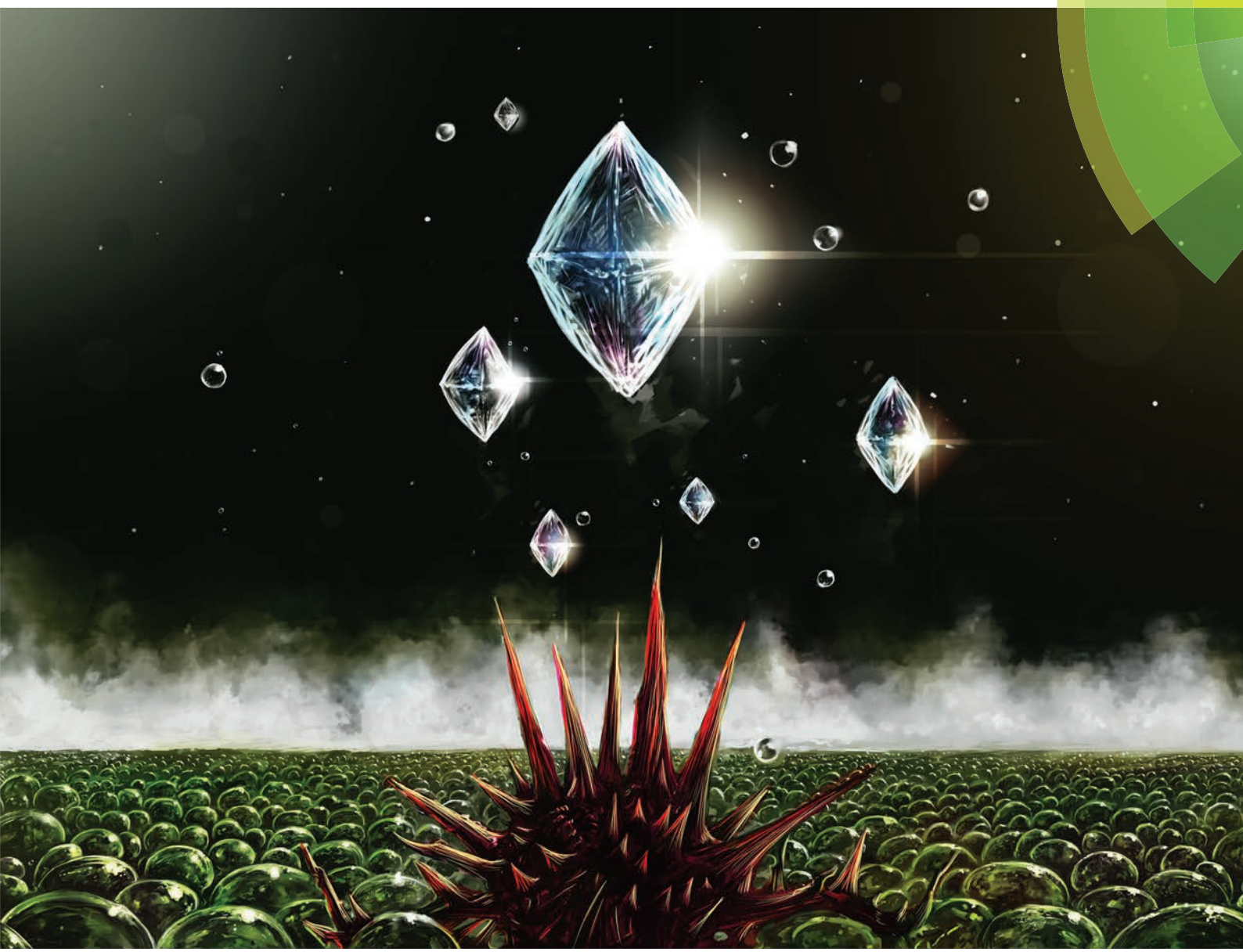

ISSN 2040-3364

ROYAL SOCIETY OF CHEMISTRY

COMMUNICATION

Petr Cigler *et al.*

Designing the nanobiointerface of fluorescent nanodiamonds: highly selective targeting of glioma cancer cells

NCNST

Nanoscale

COMMUNICATION

View Article Online
View Journal | View Issue

Cite this: *Nanoscale*, 2015, **7**, 415

Received 20th May 2014,
Accepted 20th July 2014

DOI: 10.1039/c4nr02776k

www.rsc.org/nanoscale

Designing the nanobiointerface of fluorescent nanodiamonds: highly selective targeting of glioma cancer cells†

Jitka Slegerova,[a,b] Miroslav Hajek,[a] Ivan Rehor,[a] Frantisek Sedlak,[a,b] Jan Stursa,[c] Martin Hruby[d] and Petr Cigler*[a]

Core–shell nanoparticles based on fluorescent nanodiamonds coated with a biocompatible *N*-(2-hydroxypropyl)methacrylamide copolymer shell were developed for background-free near-infrared imaging of cancer cells. The particles showed excellent colloidal stability in buffers and culture media. After conjugation with a cyclic RGD peptide they selectively targeted integrin $\alpha_v\beta_3$ receptors on glioblastoma cells with high internalization efficacy.

Optical imaging using fluorescent probes is an essential tool in contemporary biomedicine with emerging applications in areas such as cancer diagnosis. Fluorescence imaging holds advantages over other imaging methods: high sensitivity, good spatial resolution and the possibility to create environment-sensitive sensors. Although various types of molecular and nanoparticle probes have been described, they typically have limited applicability due to photobleaching, photoblinking and/or intrinsic toxicity. Fluorescent nanodiamonds (FNDs), recently introduced biocompatible near-infrared fluorescent probes, do not possess any of these disadvantages, which renders them promising nanoparticles for bioimaging applications.[1–3] Point defects in the crystal lattice structure called nitrogen-vacancy (NV) centers are responsible for the fluorescence of FNDs. NV centers are non-photobleachable and non-photoblinking fluorophores with maximum emission around 700 nm (ref. 4) and a long lifetime[5] of roughly 11–19 ns. These features have led to the use of the bright HPHT FNDs (FNDs prepared from high-pressure, high-temperature NDs) in demanding optical applications such as single particle tracking inside cells,[6] long-term *in vivo* tracking of particles,[7] tracing of neuronal processes,[8,9] revealing the relationships between the particle shape and their intracellular fate[10] and fluorescence lifetime imaging microscopy *in vitro*[11] and *in vivo*.[5] The unique sensitivity of the NV center to the electric and magnetic field was also utilized for the construction of various FND-based sensors.[12–14] Here, we show selective and highly effective targeting of glioblastoma cells (U-87 MG) expressing integrin $\alpha_v\beta_3$ using polymer-modified FND particles bearing cyclic RGD peptides.

Specific ligands attached to fluorescent probes can control probe distribution in a living system by targeting certain cellular receptors or compartments. Targeting using nanoparticles has some advantages over targeting with conventional probes. Nanoparticles have a polyvalent surface, which strengthens the binding efficacy of the targeting ligands to, for example, over-expressed receptors on cancer cells. This phenomenon is called avidity.[15,16] In contrast to free ligands, nanoparticles are not filtered through glomerular capillaries due to their size, and the efficiency of targeting is therefore increased due to the prolonged blood circulation time.[17] In cancer therapy, nanoprobes accumulate nonspecifically inside solid tumors due to the abnormal leaky tumor vasculature (Enhanced Permeation Retention, EPR effect).[18] The targeting of cancer cells by HPHT FNDs has been performed *in vitro* with various ligands such as transferrin,[19] folic acid,[20] growth hormone[21] and chlorotoxin-like peptide.[22]

The RGD recognition sequence occurs in fibronectin, fibrinogen, collagen, laminin and many other proteins present in the extracellular matrix.[23–26] This sequence specifically interacts with the integrin superfamily. The integrin receptors contain non-covalently associated α and β subunits.[15,23–26] $\alpha_v\beta_3$ integrins are overexpressed on cancer cells and endothelial cells in the tumor neovasculature. Overexpressed $\alpha_v\beta_3$ integrins are found in melanoma, breast cancer, prostate cancer, pancreatic cancer, ovarian cancer, glioblastoma and neuroblastoma.[25,27] Synthetic peptides bearing the RGD sequence and antibodies against $\alpha_v\beta_3$ integrins have been successfully used in the targeted delivery of diagnostic probes and drugs to cancer cells and tumors.[15,23] The effectiveness of targeting using the RGD motif can be improved by its cyclization. Cyclic

[a]*Institute of Organic Chemistry and Biochemistry AS CR, v.v.i., Flemingovo nam. 2, 166 10, Prague 6, Czech Republic. E-mail: cigler@uochb.cas.cz*
[b]*First Faculty of Medicine, Charles University, Katerinska 32, 121 08, Prague 2, Czech Republic*
[c]*Nuclear Physics Institute AS CR, v.v.i., 250 68 Rez near Prague, Czech Republic*
[d]*Institute of Macromolecular Chemistry AS CR, v.v.i., Heyrovskeho nam. 2, 162 06, Prague 6, Czech Republic*

† Electronic supplementary information (ESI) available: Materials and methods, colloidal stability studies and cell viability studies. See DOI: 10.1039/c4nr02776k

RGD (cRGD) peptides have higher stability, structural rigidity and better binding properties and integrin selectivity compared to linear RGD.[24,28] Peptides containing the RGD sequence are also considered promising therapeutics, because of their ability to block the integrin function.[23] For example, cilengitide, a cRGD peptide that may inhibit angiogenesis, is currently being tested in phase III clinical trials for the treatment of glioblastoma.[24]

In this work, we describe selective and specific targeting of cells derived from glioblastoma (U-87 MG; an aggressive, highly vascularized brain tumor) by FNDs. Although glioblastoma cells have been previously used as a target for cRGD-modified nanoparticles such as carbon nanotubes,[29] quantum dots[30] and gold nanoparticles,[31] effective targeting of cancer cells with directly modified FNDs is not a simple task because of their strong tendency to aggregate in biological liquids (such as buffers, media and blood).[32,33] The FND aggregates adhere non-specifically to the cell surface,[34] which can, in turn, also prevent the desired tumor selectivity due to the non-specific premature entrapment into the reticuloendothelial system. The biocompatibilization of nanodiamonds can be achieved using various direct surface modifications[35] or by polymer coatings such as polyglycerol,[36–38] poly[*N*-(2-hydroxypropyl) methacrylamide],[39] poly(ethylene oxide) (PEG),[40] PEG copolymers[41,42] and Zonyl polymer.[43] However, the targeting of a brain tumor such as glioblastoma is challenging also because of limited permeability of the blood–brain barrier (BBB). In recent studies it has been shown that BBB breakdown in tumors allows nanoparticles <200 nm in diameter to bypass the BBB and enter the brain.[44] For this type of transport a minimally adhesive nanobiointerface such as a dense PEG[44] or siRNA[45] layer is the key parameter enabling the direct treatment of brain tumors without the need for targeting moieties. Another pathway for transporting the drugs into a brain tumor is convection-enhanced delivery which can be significantly enhanced by complexation of a drug with nanodiamonds.[46]

These examples show effective ways for targeting the brain tumors based on the size and surface properties of nanoparticles. We focused here rather on controlling the selectivity of targeting using active moieties attached to FNDs and on cellular delivery of these particles in the glioblastoma model. We used our recently developed core–shell nanoparticles,[39] which comprise an FND coated with an ultra-thin silica layer and a layer of biocompatible polymethacrylamide copolymer (Scheme 1). This type of copolymer has comparable biocompatible properties as PEG[47] and serves here as a "click"-reactive interface that shields the particles against aggregation and non-specific interactions in biological environments. The layer also functions as a flexible spacer between the FND and a biomolecule.

We coated the FNDs with an ultrathin (<1 nm) silica shell grown from a mixture of tetraethoxysilane and 3-(trimethoxysilyl)propyl methacrylate using a modified Stöber procedure. A methacrylated silica layer on a FND was further coated with a copolymer of *N*-(2-hydroxypropyl)methacrylamide and *N*-propargylacrylamide. The copolymer chains were grown from the nanoparticle surface ("grafting from" approach[39]) by radical polymerization with azobis(isobutyronitrile) (AIBN) as the initiator. We focused on improving the previously described coating procedure and adjusting the reaction conditions to prefer the growth of longer polymeric chains. We increased the viscosity of the reaction mixture by performing the reaction in DMSO instead of ethanol, decreased the polymerization temperature from 70 °C to 55 °C, prolonged the time from 1 to 3 days and used a 7.5-fold higher concentration of FNDs (0.85 mg ml^{-1}) and monomers [2 M *N*-(2-hydroxypropyl)-

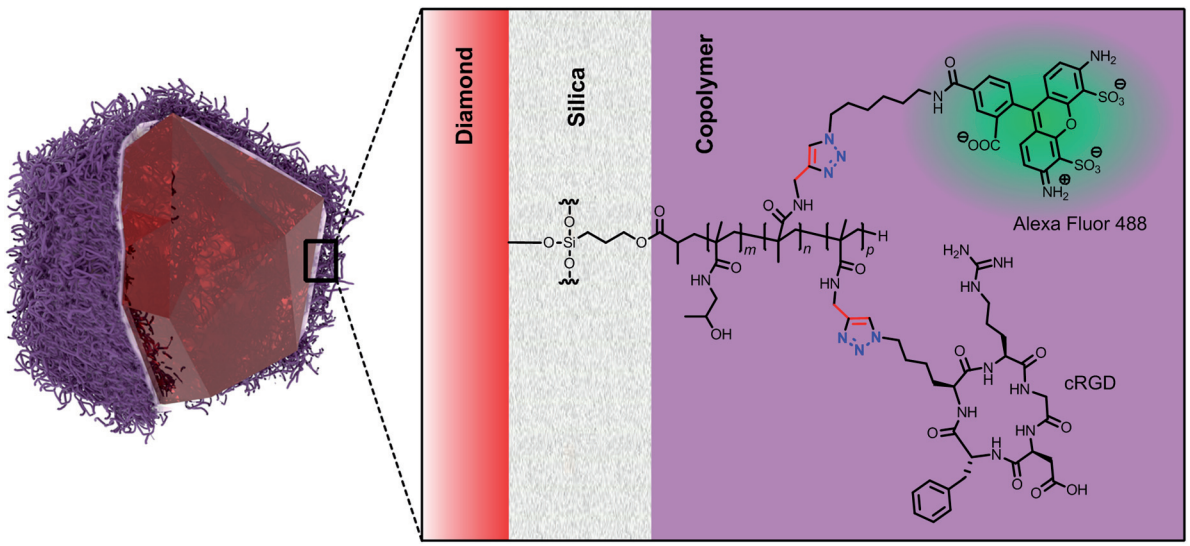

Scheme 1 Schematic structure of the fluorescent nanodiamond crystal coated with a biocompatible methacrylamide copolymer grown from an ultrathin silica shell. The copolymer bears the secondary fluorescent probe (Alexa Fluor 488) and the targeting peptide (cRGD). Both molecules were stepwise attached *via* click chemistry, providing the conjugate marked as "**FND–cRGD**" (shown here in the scheme). Reaction with only Alexa Fluor 488 provided the control particles marked in the text as "**FND**".

methacrylamide and 35 mM *N*-propargylacrylamide]. The obtained coatings further enhanced the colloidal stability of FNDs in biological environments and completely eliminated non-specific adhesion on cells. The newly prepared coated FNDs were stable even in solutions with extreme ionic strength (1 M NaCl) in contrast to our previously described polymer-coated FNDs, which were stable in NaCl solutions at concentrations up to only 0.15 M (Fig. 1S and 2S in the ESI†). In control experiments, we also did not observe any nonspecific interactions between polymer-coated FNDs and cells (see below).

To conjugate the cRGD moiety to the particles, we utilized the alkyne groups present on the copolymer chains. They are suitable for Cu(I)-catalyzed azide–alkyne cycloaddition ("click" reaction), enabling high yielding attachment of various azide-modified molecules.[48,49] The click reaction is convenient due to its high efficacy in an aqueous environment (fast kinetics under mild conditions), applicability for diverse substrates without conformational changes (from small molecules to polymers, proteins and nanoparticles) and experimental simplicity.[49–51] The click reaction is particularly attractive due to its biological inertness (bioorthogonality), in which protecting groups are avoided while specificity is ensured.[49,50]

We selected cyclic (Arg-Gly-Asp-D-Phe-Lys)-azide (Scheme 1) from a variety of cRGDs.[25] The presence of a lysine residue makes the peptide an ideal building block for further chemical conjugation reactions, such as the introduction of a bioorthogonally reactive azide group. For good targeting efficiency, the RGD peptide also needs to be exposed far from the nanoparticle surface,[52] which was here ensured by the flexibility of the polymer chains as well as by the presence of the lysine linker. The hydrodynamic diameter of the nanoparticulate bioconjugate is also kept in the range suitable for passive accumulation in solid tumor tissue due to the EPR effect or for entering the brain *via* BBB breakdown in tumors (<*ca.* 200 nm).[44] We further attached Alexa Fluor 488 to all types of particles used in the study of nanoparticles as a secondary fluorescent label because our flow cytometry setup does not allow direct observation of FND fluorescence.

We modified our polymer-coated FNDs stepwise with Alexa Fluor 488-azide and cRGD–azide using the same conjugation procedure (click chemistry). Running the reaction with a low molar excess of the first compound (Alexa Fluor 488-azide) over polymer alkyne groups resulted in substitution of only a fraction of the surface alkyne groups, providing **FNDs** (marked further in bold). This substitution resulted in approximately 300 Alexa Fluor 488 molecules per particle (*i.e.*, ~8 μmol g^{-1}) as determined spectrophotometrically. **FNDs** were then reacted with cRGD–azide, providing the **FND–cRGD** conjugate (for Experimental details, see the ESI†).

In cell experiments, we focused first on examining the potential toxicity of the particles. We tested the prepared conjugates at a concentration of 50 μg ml^{-1} on U-87 MG cells. Free cRGD (100 μg ml^{-1}) and the known apoptosis inducer staurosporine (0.3–5 μM) were used as controls (Fig. 3S and 4S in the ESI†). According to luminescent cell viability assay, **FNDs** and **FND–cRGD** did not harm cells under our experimental conditions (Fig. 1). The apparent decrease in the viability of cells incubated with free cRGD is a known consequence of cell detachment during the incubation. RGD sequences bound on a surface or macromolecule promote cell adhesion, whereas free RGD sequences in solution act as decoys, preventing adhesion.[26,53] Subsequently, we observed the interaction of particles with glioblastoma cells (U-87 MG) by flow cytometry and

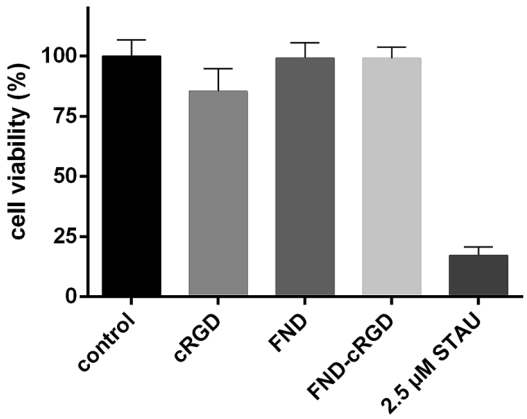

Fig. 1 Cell viability assay based on ATP quantification in cell lysates. Luminescence intensity correlates with the ATP level and thus with the quantity of metabolically active (viable) cells. Both types of polymer-coated FNDs (**FND** and **FND–cRGD** alternatives) have no impact on cell viability under the used experimental conditions. The control, FND and FND–cRGD alternatives are statistically not distinguishable among each other on the significance level α = 0.01 (ANOVA) and they are significantly different from cRGD and 2.5 μM staurosporine (α = 0.01) alternatives.

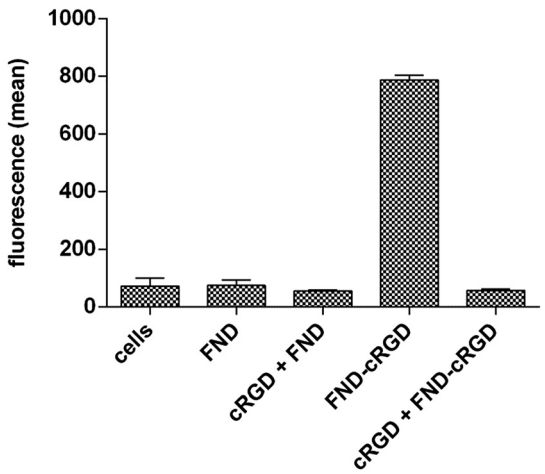

Fig. 2 Fluorescence intensity measurements of U-87 MG cells incubated with FNDs modified with cRGD (**FND–cRGD**) using flow cytometry. All types of FNDs are polymer-coated. As controls, FNDs without cRGD (**FND**) and pretreatment experiments with free cRGD peptides (cRGD + **FND** and cRGD + **FND–cRGD**) were performed. The fluorescence recorded in flow cytometry is read using Alexa Fluor 488, which is present in all types of particles. FND–cRGD specifically recognized $\alpha_v\beta_3$ integrins on U-87 MG cells. The FND + cRGD alternative is statistically significantly different from the controls (ANOVA, α = 0.01). All negative controls are statistically not distinguishable among each other on the significance level α = 0.01.

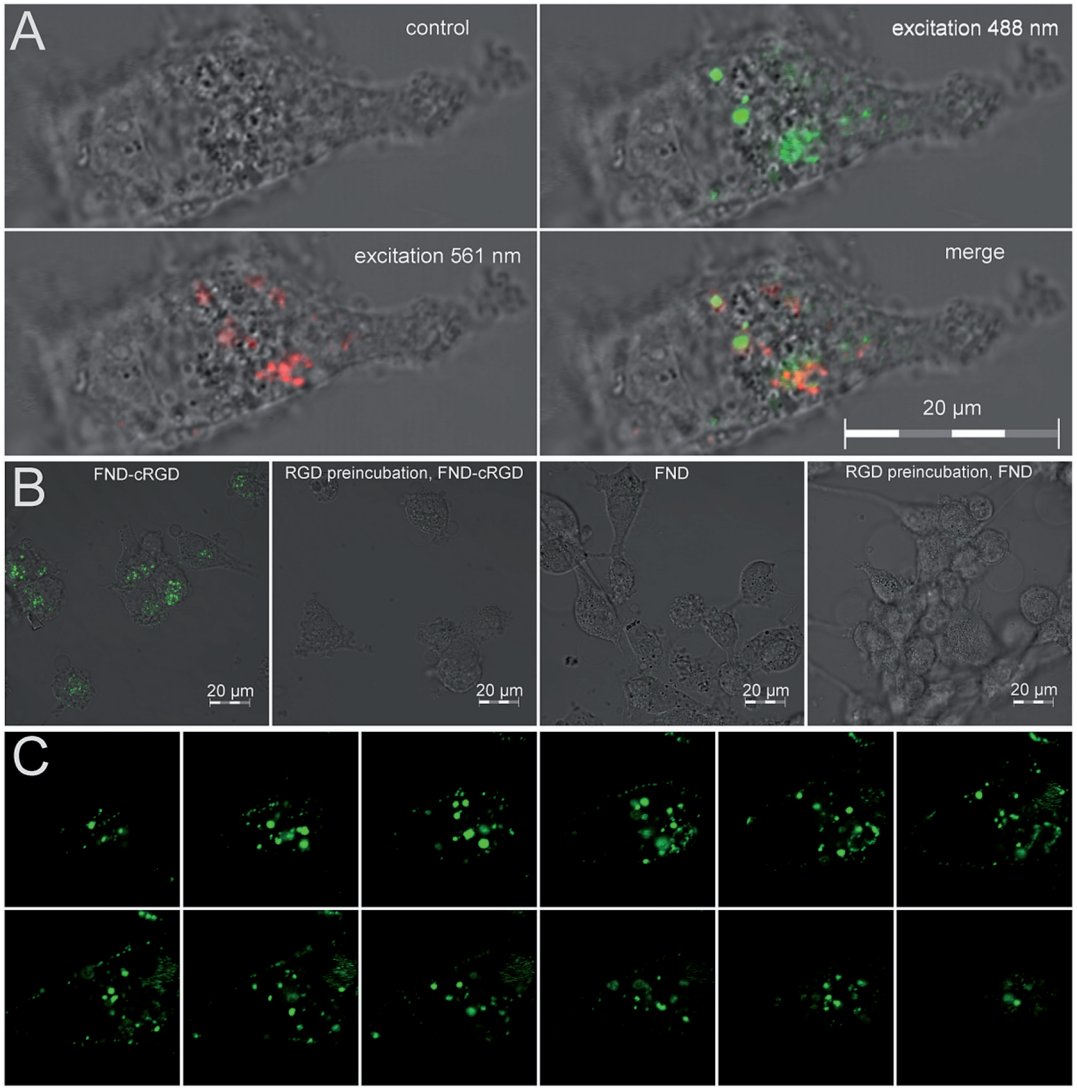

Fig. 3 Confocal fluorescence images of U-87 MG cells treated with **FND–cRGD** and **FND** nanoparticles (all particles are polymer-coated). (A) Measurement of **FND–cRGD** in cells using fluorescence of Alexa Fluor 488 and FNDs' fluorescence (excitation at 488 and 561 nm, respectively). The last picture shows merged results from both channels. The confocal images were taken at the same focal plane. The time between the measurements of Alexa Fluor 488 fluorescence and FND's intrinsic fluorescence was due to extensive photobleaching on a scale of tens of minutes. (B) Merged fluorescence and bright-field images of cells treated with **FND–cRGD** and **FND** nanoparticles with or without pretreatment with a free cRGD peptide. Only **FND–cRGD** without pretreatment was found inside the cells. The images were recorded using the Alexa Fluor 488 channel. (C) Cross-section measurement of cells treated with **FND–cRGD** shows that particles are present inside the cell. Images were recorded with a 1.5 μm step in the vertical direction and presented from left to right and top to bottom with a 28 × 28 μm field of view. The images were recorded using the Alexa Fluor 488 channel.

confocal microscopy. Either **FND** or **FND–cRGD** at a final concentration of 50 μg ml^{-1} was incubated with the cells for 1 hour.

The strong affinity of **FND–cRGD** over **FND** to U-87 MG cells was revealed by flow cytometry, which shows 12-fold higher fluorescence upon nanoparticle binding (Fig. 2; for histograms see Fig. 5S†). Differences in the surface compositions of **FND** and **FND–cRGD** (*i.e.*, the presence of a relatively hydrophobic cyclic peptide) can lead to different surface properties that are not related to integrin binding specificity. We tested therefore this possible behavior using a free cRGD peptide added in excess during pretreatment (30 min, 100 μg ml^{-1}), which saturates the RGD-binding sites (*i.e.*, $\alpha_v\beta_3$ integrins). We observed no significant differences between **FND** and **FND–cRGD** affinities when cells were pretreated with cRGD. This clearly indicates that **FND–cRGD** particles use integrins as their receptors to bind the cells and that the interaction is highly specific (Fig. 2).

We were further interested in testing the relevance of flow cytometry experiments recorded using Alexa Fluor 488 fluorescence by confocal microscopy, so we studied the colocalization of intrinsic FND and Alexa 488 fluorescence for **FND–cRGD** particles (Fig. 3A). Notably, we took advantage of the extreme photostability of FND fluorescence to record confocal images before and after photobleaching of Alexa Fluor

488 fluorescence (and cell autofluorescence). This procedure enabled background-free imaging of FND fluorescence. A similar pattern of bright spots in the merged picture (from both channel detections) showed that Alexa Fluor 488 is bound to the particles. The quantification of the colocalization data suggests that FND's fluorescence almost completely overlaps Alexa Fluor 488 fluorescence (Manderson M = 0.93) and Alexa Fluor 488 fluorescence shows also a strong overlap with FND's fluorescence (Manderson M = 0.78). These data confirmed the relevance of flow cytometry for quantification of the particle interaction with cells.

Finally, we focused on supporting the results from flow cytometry experiments using confocal microscopy and on determination whether the **FND–cRGD** particles enter the cell or remain bound to the surface. Complementary to our flow cytometry data, confocal microscopy also showed no interaction between non-targeted **FND** particles and U-87 MG cells, while the **FND–cRGD** were bound to the cells (Fig. 3B). Using confocal microscopy cross-section measurements, we found that **FND–cRGD** is localized inside the cells (Fig. 3C). This finding corresponds to the results from other studies in which internalization *via* receptor-mediated endocytosis of various RGD-targeted nanocarriers was observed.[24] Notably, a similar and effective approach as has been demonstrated here was published during revisions of this paper for targeting of the U-87 MG cells by RGD-modified polyglycerol-coated FNDs.[37]

Conclusions

We designed and prepared a novel type of FND-based nanoparticles that target glioma cells with unprecedented efficiency and specificity. The nanoparticles consist of an FND core coated with an ultra-thin silica layer and a biocompatible *N*-(2-hydroxypropyl)methacrylamide copolymer shell bearing cRGD peptides. This ligand on the nanoparticle surface is a tight-binder of integrin $\alpha_v\beta_3$ receptors, which are overexpressed on this type of cancer cells. Upon selective recognition and binding to $\alpha_v\beta_3$ receptors, the particles are internalized and localized inside the cell. Thanks to their extreme photostability, the particles can be used for background-free near-infrared imaging of cancer cells for an unlimited period of time.

Acknowledgements

The work was supported by GAČR project P108/12/0640. Irradiation of NDs was carried out at the CANAM infrastructure of the NPI AS CR Rez supported through MŠMT project no. LM2011019. The work of M. H. (IOCB AS CR) was supported by Project NPU I, LO 1302 from the Ministry of Education, Youth and Sports.

References

1 E. K.-H. Chow and D. Ho, *Sci. Transl. Med.*, 2013, **5**, 216rv4.
2 J. Slegerova, I. Rehor, J. Havlik, H. Raabova, E. Muchova and P. Cigler, in *Intracellular Delivery II*, ed. A. Prokop, Y. Iwasaki and A. Harada, Springer, Netherlands, 2014, pp. 363–401.
3 Y. Y. Hui, C. L. Cheng and H. C. Chang, *J. Phys. D: Appl. Phys.*, 2010, **43**, 374021.
4 S.-J. Yu, M.-W. Kang, H.-C. Chang, K.-M. Chen and Y.-C. Yu, *J. Am. Chem. Soc.*, 2005, **127**, 17604–17605.
5 Y. Kuo, T.-Y. Hsu, Y.-C. Wu, J.-H. Hsu and H.-C. Chang, *Proc. SPIE*, 2013, **8635**, 863503–863507.
6 Y.-R. Chang, H.-Y. Lee, K. Chen, C.-C. Chang, D.-S. Tsai, C.-C. Fu, T.-S. Lim, Y.-K. Tzeng, C.-Y. Fang, C.-C. Han, H.-C. Chang and W. Fann, *Nat. Nanotechnol.*, 2008, **3**, 284–288.
7 V. Vaijayanthimala, P.-Y. Cheng, S.-H. Yeh, K.-K. Liu, C.-H. Hsiao, J.-I. Chao and H.-C. Chang, *Biomaterials*, 2012, **33**, 7794–7802.
8 T.-C. Hsu, K.-K. Liu, H.-C. Chang, E. Hwang and J.-I. Chao, *Sci. Rep.*, 2014, **4**, 5004.
9 X. L. Le, A.-M. Lepagnol-Bestel, M.-P. Adam, A. Thomas, G. Dantelle, C.-C. Chang, N. Mohan, H.-C. Chang, F. Treussart and M. Simonneau, *Proc. SPIE*, 2012, **8232**, 823203.
10 Z. Chu, S. Zhang, B. Zhang, C. Zhang, C.-Y. Fang, I. Rehor, P. Cigler, H.-C. Chang, G. Lin, R. Liu and Q. Li, *Sci. Rep.*, 2014, **4**, 4495.
11 O. Faklaris, D. Garrot, V. Joshi, F. Druon, J. P. Boudou, T. Sauvage, P. Georges, P. A. Curmi and F. Treussart, *Small*, 2008, **4**, 2236–2239.
12 A. Ermakova, G. Pramanik, J.-M. Cai, G. Algara-Siller, U. Kaiser, T. Weil, Y.-K. Tzeng, H. C. Chang, L. P. McGuinness, M. B. Plenio, B. Naydenov and F. Jelezko, *Nano Lett.*, 2013, **13**, 3305–3309.
13 V. Petrakova, A. Taylor, I. Kratochvilova, F. Fendrych, J. Vacik, J. Kucka, J. Stursa, P. Cigler, M. Ledvina, A. Fiserova, P. Kneppo and M. Nesladek, *Adv. Funct. Mater.*, 2012, **22**, 812–819.
14 L. P. McGuinness, Y. Yan, A. Stacey, D. A. Simpson, L. T. Hall, D. Maclaurin, S. Prawer, P. Mulvaney, J. Wrachtrup, F. Caruso, R. E. Scholten and L. C. L. Hollenberg, *Nat. Nanotechnol.*, 2011, **6**, 358–363.
15 E. Ruoslahti, S. N. Bhatia and M. J. Sailor, *J. Cell Biol.*, 2010, **188**, 759–768.
16 X. Montet, M. Funovics, K. Montet-Abou, R. Weissleder and L. Josephson, *J. Med. Chem.*, 2006, **49**, 6087–6093.
17 K. Temming, R. M. Schiffelers, G. Molema and R. J. Kok, *Drug Resist. Updates*, 2005, **8**, 381–402.
18 R. K. Jain and T. Stylianopoulos, *Nat. Rev. Clin. Oncol.*, 2010, **7**, 653–664.
19 M. F. Weng, S. Y. Chiang, N. S. Wang and H. Niu, *Diamond Relat. Mater.*, 2009, **18**, 587–591.
20 B. Zhang, Y. Li, C.-Y. Fang, C.-C. Chang, C.-S. Chen, Y.-Y. Chen and H.-C. Chang, *Small*, 2009, **5**, 2716–2721.
21 C.-Y. Cheng, E. Perevedentseva, J.-S. Tu, P.-H. Chung, C.-L. Cheng, K.-K. Liu, J.-I. Chao, P.-H. Chen and C.-C. Chang, *Appl. Phys. Lett.*, 2007, **90**, 163903.

22 Y. Fu, N. An, S. Zheng, A. Liang and Y. Li, *Diamond Relat. Mater.*, 2012, **21**, 73–76.
23 J. B. Delehanty, K. Boeneman, C. E. Bradburne, K. Robertson, J. E. Bongard and I. L. Medintz, *Ther. Delivery*, 2010, **1**, 411–433.
24 F. Danhier, A. L. Breton and V. Préat, *Mol. Pharm.*, 2012, **9**, 2961–2973.
25 S. Liu, *Bioconjugate Chem.*, 2009, **20**, 2199–2213.
26 E. Ruoslahti, *Annu. Rev. Cell Dev. Biol.*, 1996, **12**, 697–715.
27 Z. Cheng, A. Al Zaki, J. Z. Hui, V. R. Muzykantov and A. Tsourkas, *Science*, 2012, **338**, 903–910.
28 S. Liu, *Mol. Pharm.*, 2006, **3**, 472–487.
29 B. R. Smith, C. Zavaleta, J. Rosenberg, R. Tong, J. Ramunas, Z. Liu, H. Dai and S. S. Gambhir, *Nano Today*, 2013, **8**, 126–137.
30 J. Gao, K. Chen, R. Xie, J. Xie, Y. Yan, Z. Cheng, X. Peng and X. Chen, *Bioconjugate Chem.*, 2010, **21**, 604–609.
31 M. Luna-Gutiérrez, G. Ferro-Flores, B. Ocampo-García, N. Jiménez-Mancilla, E. Morales-Avila, L. De León-Rodríguez and K. Isaac-Olivé, *J. Labelled Compd. Radiopharm.*, 2012, **55**, 140–148.
32 S. A. Dahoumane, M. N. Nguyen, A. Thorel, J.-P. Boudou, M. M. Chehimi and C. Mangeney, *Langmuir*, 2009, **25**, 9633–9638.
33 V. K. A. Sreenivasan, E. A. Ivukina, W. Deng, T. A. Kelf, T. A. Zdobnova, S. V. Lukash, B. V. Veryugin, O. A. Stremovskiy, A. V. Zvyagin and S. M. Deyev, *J. Mater. Chem.*, 2011, **21**, 65.
34 I. Rehor, J. Slegerova, J. Kucka, V. Proks, V. Petrakova, M.-P. Adam, F. Treussart, S. Turner, S. Bals, P. Sacha, M. Ledvina, A. M. Wen, N. F. Steinmetz and P. Cigler, *Small*, 2014, **10**, 1029.
35 A. Krueger and D. Lang, *Adv. Funct. Mater.*, 2012, **22**, 890–906.
36 L. Zhao, T. Takimoto, M. Ito, N. Kitagawa, T. Kimura and N. Komatsu, *Angew. Chem., Int. Ed.*, 2011, **50**, 1388–1392.
37 L. Zhao, Y.-H. Xu, H. Qin, S. Abe, T. Akasaka, T. Chano, F. Watari, T. Kimura, N. Komatsu and X. Chen, *Adv. Funct. Mater.*, 2014, DOI: 10.1002/adfm.201304298.
38 J.-P. Boudou, M.-O. David, V. Joshi, H. Eidi and P. A. Curmi, *Diamond Relat. Mater.*, 2013, **38**, 131–138.
39 I. Rehor, H. Mackova, S. K. Filippov, J. Kucka, V. Proks, J. Slegerova, S. Turner, G. Van Tendeloo, M. Ledvina, M. Hruby and P. Cigler, *ChemPlusChem*, 2014, **79**, 21–24.
40 T. Takimoto, T. Chano, S. Shimizu, H. Okabe, M. Ito, M. Morita, T. Kimura, T. Inubushi and N. Komatsu, *Chem. Mater.*, 2010, **22**, 3462–3471.
41 J. W. Lee, S. Lee, S. Jang, K. Y. Han, Y. Kim, J. Hyun, S. K. Kim and Y. Lee, *Mol. BioSyst.*, 2013, **9**, 1004.
42 H. B. Man, R. Lam, M. Chen, E. Osawa and D. Ho, *Phys. Status Solidi A*, 2012, **209**, 1811–1818.
43 L. Marcon, Z. Kherrouche, J. Lyskawa, D. Fournier, D. Tulasne, P. Woisel and R. Boukherroub, *Chem. Commun.*, 2011, **47**, 5178–5180.
44 E. A. Nance, G. F. Woodworth, K. A. Sailor, T.-Y. Shih, Q. Xu, G. Swaminathan, D. Xiang, C. Eberhart and J. Hanes, *Sci. Transl. Med.*, 2012, **4**, 149ra119.
45 S. A. Jensen, E. S. Day, C. H. Ko, L. A. Hurley, J. P. Luciano, F. M. Kouri, T. J. Merkel, A. J. Luthi, P. C. Patel, J. I. Cutler, W. L. Daniel, A. W. Scott, M. W. Rotz, T. J. Meade, D. A. Giljohann, C. A. Mirkin and A. H. Stegh, *Sci. Transl. Med.*, 2013, **5**, 209ra152.
46 G. Xi, E. Robinson, B. Mania-Farnell, E. F. Vanin, K.-W. Shim, T. Takao, E. V. Allender, C. S. Mayanil, M. B. Soares, D. Ho and T. Tomita, *Nanomedicine: Nanotechnology, Biology and Medicine*, 2014, **10**, 381–391.
47 J. Kopecek, *Adv. Drug Delivery Rev.*, 2013, **65**, 49–59.
48 V. Hong, S. I. Presolski, C. Ma and M. G. Finn, *Angew. Chem., Int. Ed.*, 2009, **48**, 9879–9883.
49 E. Lallana, A. Sousa-Herves, F. Fernandez-Trillo, R. Riguera and E. Fernandez-Megia, *Pharm. Res.*, 2012, **29**, 1–34.
50 G. von Maltzahn, Y. Ren, J.-H. Park, D.-H. Min, V. R. Kotamraju, J. Jayakumar, V. Fogal, M. J. Sailor, E. Ruoslahti and S. N. Bhatia, *Bioconjugate Chem.*, 2008, **19**, 1570–1578.
51 D. L. J. Thorek, D. R. Elias and A. Tsourkas, *Mol. Imaging*, 2009, **8**, 221–229.
52 U. Hersel, C. Dahmen and H. Kessler, *Biomaterials*, 2003, **24**, 4385–4415.
53 E. Ruoslahti and M. D. Pierschbacher, *Science*, 1987, **238**, 491–497.

